Role of the Membrane for Mechanosensing by Tethered Channels

Benedikt Sabass and Howard A. Stone

Phys. Rev. Lett. **116**, 258101 — Published 20 June 2016

DOI: 10.1103/PhysRevLett.116.258101

Role of the membrane for mechanosensing by tethered channels

Benedikt Sabass and Howard A. Stone
Department of Mechanical and Aerospace Engineering, Princeton University, Princeton, USA

Biologically important membrane channels are gated by force at attached tethers. Here, we generically characterize the non-trivial interplay of force, membrane tension, and channel deformations that can affect gating. A central finding is that minute conical channel deformation under force leads to significant energy release during opening. We also calculate channel-channel interactions and show that they can amplify force sensitivity of tethered channels.

PACS numbers: 87.16.dm, 87.14.ep, 87.15.kt

Introduction.– The conversion of mechanical signals to a biochemical response is essential for living matter. One important class of mechanosensing proteins are membrane channels that are required for numerous biological functions, such as hearing [1], the sense of touch [2], or regulation of intracellular mechanics [3]. Recently, mechanosensitive channels have received considerable scientific attention, mostly with a focus on tension-sensing [4, 5]. A fundamental insight was that membrane energy is sufficient to cause channel deformations that lead to gating, i.e. opening or closing of the channel. As reviewed in [6], the deformation modes include conical shape changes [7–11], radial expansion [12–15], or changes in channel hydrophobic thickness [16, 17]. However, in many cases the channels are directly tethered to cytoskeletal or extracellular structures, which allow a direct transmission of mechanical force [18–20].

One example of a tethered channel is the DEG/ENaC complex, which conveys touch sensing in C. elegans [21]. Here, an ion channel is likely opened by mechanical interaction with intracellular or extracellular proteins [22]. Further examples of tethered channels are force-sensitive TRP channels that possess intracellular ankyrin domains. Ankyrin repeats are proposed to function as "gating springs" that convey force [23–26]. These tethers have an estimated stiffness of 1 pN/nm and a working range on the order of 10 nm. Thus, forces are estimated to be around 10 pN [27, 28]. The pN force scale is also confirmed by experiments [3]. Since the observed gating is stochastic [26, 29], energy barriers are expected to be comparable to the thermal energy.

A role of the membrane has been experimentally verified for tethered TRPA1 channels. Here, gating depends robustly and asymmetrically on membrane curvature that is induced by amphipathic molecules, partitioning either in the inner or outer leaflet [30]. Furthermore, GsMTx-4, a toxin that inhibits tension-activated channels through perturbing the bilayer [31], causes gating of TRPA1 [30]. In spite of experimental evidence, a theoretical analysis of the role of the membrane for tethered channels is lacking, and this is the focus of this Letter.

In quasi-equilibrium, channel gating is governed by an energy $\mathcal{F}$, which depends on the internal molecular state and on the deformation of the membrane around the channel. Thus, $\mathcal{F} = \mathcal{F}_{\rm int} + \mathcal{F}_{\rm m}$. The internal energy $\mathcal{F}_{\rm int}$ is determined by structural details, whose characterization requires intricate molecular dynamics studies [32]. In contrast, the membrane energy $\mathcal{F}_{\rm m}$ always affects gating if sufficient channel shape changes occur [6]. Focusing on generic principles, we study how force and the membrane affect two main channel deformation modes, namely conical deformation and radial expansion.

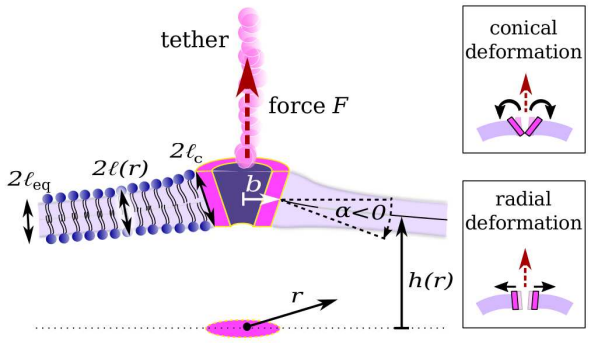

FIG. 1. Model for a tethered channel embedded in a lipid bilayer. Variables are defined in the main text. The channel shape changes either by conical deformation where the angle α varies or by radial deformation with variation of b.

Calculation of membrane energy.– We consider a radially symmetric channel that is placed on the centerline of a cylindrical system with radial coordinate r (Fig. 1). A constant vertical force F is exerted on the channel, with signs chosen such that $F > 0$ is directed upwards. The channel radius is denoted by b; typically $b \simeq 3\,$nm. A conical channel shape is characterized by the angle α, with signs chosen such that $\alpha > 0$ corresponds to a channel with small side pointing upwards. The channel is surrounded by a fluid lipid bilayer. The height of the center of the bilayer above a reference plane is denoted by $h(r)$, with $h(0)$ being the height at the channel center. The bilayer thickness is denoted by $2\ell(r)$. Hydrophobic properties of the channel can force the membrane leaflets to splay, leading to a perturbation of the equilibrium leaflet thickness $u(r) \equiv \ell - \ell_{\rm eq}$. Typically, $\ell_{\rm eq} \simeq 1.75\,$nm [33].

The linearized membrane deformation energy is [16, 34]

$$\mathcal{F}_\mathrm{m} = \int \left[\frac{\kappa_\mathrm{b}}{2}(\nabla^2 u)^2 + \frac{\kappa_\mathrm{a}}{2}\left(\frac{u}{\ell_\mathrm{eq}}\right)^2 + \frac{\gamma}{2}(\nabla u)^2 \right] \mathrm{d}^2 r + \int \left[\frac{\kappa_\mathrm{b}}{2}(\nabla^2 h)^2 + \frac{\gamma}{2}(\nabla h)^2 \right] \mathrm{d}^2 r + \gamma \int \mathrm{d}^2 r - F h(0), \tag{1}$$

where the surface integral extends over the entire reference plane outside the channel. Neglecting shear forces between the leaflets, we assume that the bending modulus κ_b is the same for thickness perturbations u and height perturbations h. Typically, $\kappa_\mathrm{b} \simeq 25\,\mathrm{k_B T}$ [33]. Changes of membrane thickness are penalized by the term $\sim \kappa_\mathrm{a} u^2$, where $\kappa_\mathrm{a} \simeq 40\,\mathrm{k_B T/nm^2}$ [16, 33]. Tension γ maintains constant area of both leaflets. For eukaryotes, tension is usually low, $\gamma \simeq 10^{-3}\,\mathrm{k_B T/nm^2}$ [35], and large amounts of excess area are believed to lead to constant tension [36]. Therefore, in line with previous research [37], we assume that the force F does not appreciably affect membrane tension. A large natural scale for tension can be fixed by combining the bending modulus and channel radius as $\gamma_S \equiv \kappa_\mathrm{b}/b^2$; typically $\gamma_S \simeq 2.7\,\mathrm{k_B T/nm^2} \gg \gamma$.

Depending on membrane composition, the orientational ordering of lipids may affect deformations on the nanometer scale [38–40], which may require further terms in Eq. (1) [41–49]. The influence of lipid tilt is analyzed in the Supplemental Material. Furthermore, elastic interactions between the membrane and environment may change $\mathcal{F}_\mathrm{m}$. An elastically supported membrane is studied in the Supplemental Material.

The membrane height $h(r)$ is locally determined by a combined effect of tension and bending, which allows the introduction of a characteristic lengthscale as

$$\xi^{-1} \equiv \sqrt{\kappa_\mathrm{b}/\gamma}. \tag{2}$$

Typical values of the lengthscale are $\xi^{-1} \simeq [5 \ldots 500]\,\mathrm{nm}$, which is larger than the channel radius b. A variation of Eq. (1) yields equilibrium equations determining $h(r)$ as

$$\nabla^2(\nabla^2 - \xi^2)h = 0, \tag{3a}$$

$$F = 2\pi b \kappa_\mathrm{b} \partial_r \left(\nabla^2 h - \xi^2 h\right)|_b, \qquad \partial_r h|_b = \alpha, \tag{3b}$$

where the boundary conditions involving F and α fix the height and contact angle at the channel. Far away from the channel, at $r = L \gg b$, we assume $h|_L = 0$.

A variation of Eq. (1) also yields the equation determining thickness perturbations $u(r)$. If the membrane leaflets are fixed to the channel walls by chemical interactions, the force F does not change the thickness perturbation around the channel. Then we have

$$(\nabla^2 - \eta_-^2)(\nabla^2 - \eta_+^2)u = 0, \tag{4a}$$

$$u|_b = (\ell_c - \ell_\mathrm{eq}), \qquad \partial_r u|_b = 0, \tag{4b}$$

where $\eta_\pm^2 \equiv \left(\xi^2 \pm \sqrt{\xi^4 - 4\kappa_\mathrm{a}/(\ell_\mathrm{eq}^2 \kappa_\mathrm{b})}\right)/2$ and $\partial_r u|_L = 0$, $u|_L = 0$. The lengthscale of thickness perturbations is $\bar{\eta}^{-1} \equiv (\eta_+^{-1} + \eta_-^{-1})$, which is about 1.5 nm [50, 51].

Once u and h are calculated, the energy $\mathcal{F}_\mathrm{m}$ results from Eq. (1) [34]. Due to its two-dimensional nature, $\mathcal{F}_\mathrm{m}$ displays a logarithmic divergence with system size L. However, this divergent energy does not depend on channel shape parameters, and is thus immaterial for gating. We remove the divergence and other constants by defining $\tilde{\mathcal{F}}_\mathrm{m} \equiv \mathcal{F}_\mathrm{m} + F^2\,[\Gamma_e + \log(\xi L/2)]/(4\pi\gamma)$, where $\Gamma_e = 0.577\ldots$ is the Euler-Mascheroni constant. Since usually $b\xi < 1$, the membrane energy can be expanded up to $O((b\xi)^3)$ to yield a transparent formula

$$\tilde{\mathcal{F}}_\mathrm{m} \approx d^2 b - \gamma\pi b^2(1 - \alpha^2 X) + b\alpha F X + \frac{b^2(F + 2b\alpha\gamma\pi)^2 Y}{4\kappa_\mathrm{b}\pi}, \tag{5}$$

where $d^2 \equiv \pi\kappa_\mathrm{b}(\ell_c - \ell_\mathrm{eq})^2 \eta_+\eta_-(\eta_+ + \eta_-)$ [34]. Further constants are $X \equiv -\Gamma_e - \log[b\xi/2]$ and $Y \equiv (1 + 2X + 2X^2)/4$; X and Y are both positive for $b\xi < 1$.

Eq. (5) allows to calculate how membrane energy changes with channel shape. The first term $d^2 b$ results from membrane thickness perturbations u around the channel. This energy is independent of F and penalizes radial expansion. Note that d^2 may change with channel deformation if the hydrophobic thickness varies. Other small-scale effects, such as tilt of the lipids, bending of their acyl chains, and the detailed channel structure may also affect d^2. The second term in Eq. (5) results from membrane tension. This energy contribution usually decreases with radius b, except when the channel is very conical $\alpha^2 X > 1$. The two last terms in Eq. (5) contain the effect of the force. An important role of the conical shape is evident from the occurrence of α in both terms. In the following, we use $\mathcal{F}_\mathrm{m}$ to analyze the energetics of channel deformation.

Conical deformation.– We first study a change of the conical angle α. For an initially closed channel with $\alpha = \alpha_c$, the angle may change during gating as $\alpha_c \to \alpha_c + \Delta\alpha$. The membrane favors such a channel deformation if the energy is reduced as $\mathcal{F}_\mathrm{m}(\alpha_c + \Delta\alpha) - \mathcal{F}_\mathrm{m}(\alpha_c) < 0$. Fig. 2a indicates how $\mathcal{F}_\mathrm{m}$ changes with $\Delta\alpha$. A force F tilts the energy function, making conical deformation favorable in one angular direction and unfavorable in the other. For physiologically low membrane tension $< 10^{-1}\gamma_S$, Fig. 2a illustrates that membrane energy varies almost linearly with $\Delta\alpha$. In this case, Eq. (5) yields

$$\tilde{\mathcal{F}}_\mathrm{m}(\Delta\alpha) - \tilde{\mathcal{F}}_\mathrm{m}(0) \simeq bFX\,\Delta\alpha. \tag{6}$$

Using this simple formula with typical values $F = 10\,\mathrm{pN}$, $b = 3\,\mathrm{nm}$, $\xi^{-1} = 50\,\mathrm{nm}$, we find that an angular deformation of $\Delta\alpha = 3^\circ$ corresponds to an energy change of $\simeq 1\,\mathrm{k_B T}$. Hence, minute molecule deformations of even $1\,\mathring{A}$ significantly affect the membrane energy in the presence of a force.

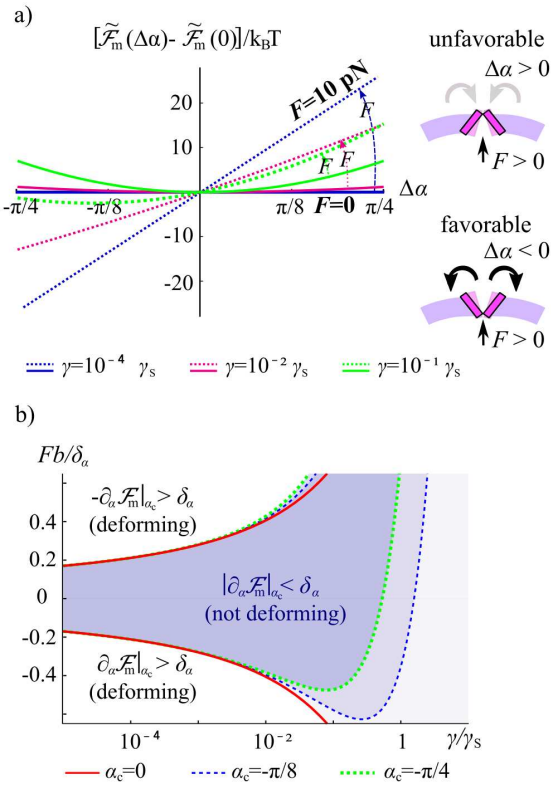

FIG. 2. a) Change of membrane energy with conical angle $\Delta\alpha$ when the channel is initially cylindrical ($\alpha_c = 0$). Force $F > 0$ tilts the function to make deformations $\Delta\alpha < 0$ energetically favorable (dotted lines). b) Lines of threshold forces $F^*(\gamma, \alpha_c)$ that allow opening against an internal molecular resistance δ_α/b. Note the amplification of applied force $F^* b/\delta_\alpha < 1$, which results from membrane leverage. Representative parameters: $b = 3\,\mathrm{nm}$, $\kappa_b = 25\,k_BT$, $\delta_\alpha = 180\,k_BT/\pi$.

Next, we assume that the molecular channel structure poses an energetic barrier to conical deformations. Without knowledge of details, the resistance to deformation can be described through an energy scale $\delta_\alpha \equiv \partial_\alpha \mathcal{F}_{\rm int}|_{\alpha_c}$. Applying force to a channel causes conical deformations if the net energy is reduced $-|\partial_\alpha \mathcal{F}_m|_{\alpha_c} + \delta_\alpha \le 0$. Force thresholds F^* for the occurrence of conical deformation are thus calculated from the criterion $|\partial_\alpha \mathcal{F}|_{\alpha_c} = \delta_\alpha$. Fig. 2b displays lines for F^* that separate parameter regions where conical deformation occurs. Note the scale on the ordinate $Fb/\delta_\alpha < 1$, which means that a small applied force F can overcome larger resisting internal force δ_α/b and thus cause conical deformation.

To understand this amplification of the force F we use Eq. (6) and estimate $|\partial_\alpha \mathcal{F}_m|_{\alpha_c} \sim bFX$. Equating membrane deformation energy with internal energy $|\partial_\alpha \mathcal{F}_m|_{\alpha_c} = \delta_\alpha$, the threshold force follows as $F^* \sim \delta_\alpha/(bX)$. Thus, forces result from dividing the internal energy scale δ_α by a lever arm length $bX \sim -b\log(b\xi)$, which includes the large scale membrane deformation. Since X depends only logarithmically on γ and κ_b, threshold forces are relatively robust against variation of these membrane properties.

In Fig. 2b, data for $\alpha_c \neq 0$ illustrates deformation of a channel that already has a conical shape. For small tension, $\gamma/\gamma_S \lesssim 10^{-2}$, all curves lie on top each other since force thresholds F^* are not affected by the initial conical angle α_c. On the other hand, strong tension can deform a channel with $\alpha_c \neq 0$ even when $F = 0$.

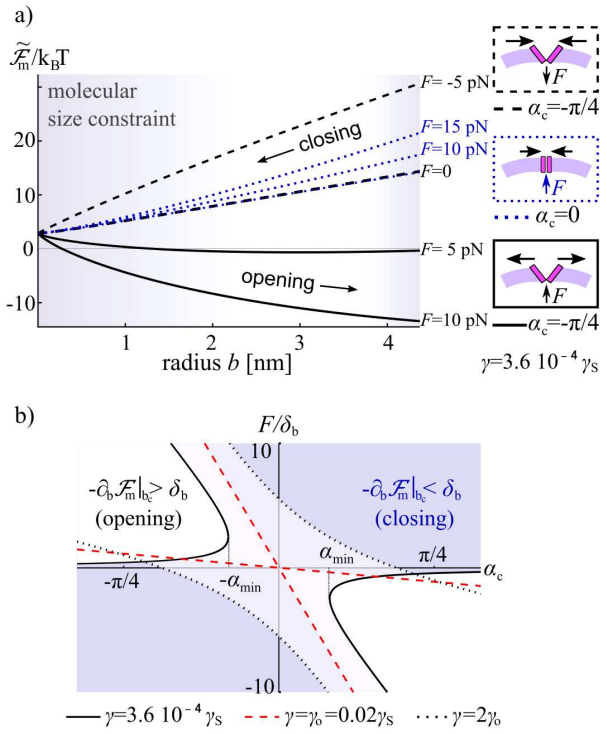

FIG. 3. a) Membrane energy $\tilde{\mathcal{F}}_m$ vs. channel radius b. Opening is favored when $\partial_b \tilde{\mathcal{F}}_m < 0$. For $F = 0$, an assumed hydrophobic mismatch $(\ell_c - \ell_{eq}) = 0.2\,\mathrm{nm}$ dominates $\mathcal{F}_m$, thus $\partial_b \tilde{\mathcal{F}}_m > 0$. $\partial_b \tilde{\mathcal{F}}_m < 0$ requires a conical channel with $\alpha_c F < 0$. b) Lines of threshold forces $F^{**}(\gamma, \alpha_c)$ at which radial expansion becomes possible. Full lines: For $\gamma < \gamma_o$, threshold forces describe hyperbolic regions where opening occurs when $|\alpha_c| > |\alpha_{min}|$. Dashed and dotted lines: When $\gamma \ge \gamma_o$, membrane tension is sufficient to radially open a channel at $\alpha_c = 0$. In b) $(\ell_c - \ell_{eq}) = 0$. Representative parameters: $\kappa_b = 25\,k_BT$, $\kappa_a = 40\,k_BT/\mathrm{nm}^2$, $b_c = 3\,\mathrm{nm}$, $\delta_b = 1\,k_BT/\mathrm{nm}$.

Radial deformation.– Channel gating may lead to an increase of the radius b. However, if $\partial_b \tilde{\mathcal{F}}_m(b) > 0$, membrane deformation does not favor this expansion. Fig. 3a shows the dependence of membrane energy $\tilde{\mathcal{F}}_m$ on radius b for typical parameter values. Clearly, $\partial_b \tilde{\mathcal{F}}_m(b) < 0$ only occurs for a pronounced conical shape. For small angles $\alpha_c \simeq 0$ or large F, force always favor radial closure of the channel.

Analogous to the analysis of conical deformations, we next assume that the channel itself resists radial deformation through an internal force $\delta_b \equiv \partial_b \mathcal{F}_{\rm int}|_{b_c}$, which is caused by conformational changes. Threshold forces

for radial opening F^{**} are calculated from the condition $\partial_b \mathcal{F}_\mathrm{m}|_{b_c} + \delta_b = 0$. Fig. 3b displays thresholds F^{**} that separate regions of parameters (F, α_c) where channels are open or closed. The shape of these regions depends on tension γ. The critical tension $\gamma_o \equiv (d^2 + \delta_b)/(2\pi b_c)$, which opens a cylindrical channel $\alpha_c = 0$ when $F = 0$, allows discrimination of two regimes. For $\gamma > \gamma_o$, we find one central parameter region where the channel is held open by tension. When $\gamma < \gamma_o$, two hyperbolic regions exist where force can lead to radial opening when pushing towards the larger side of a conical channel. These hyperbolic regions are limited by finite angles $|\alpha_\mathrm{min}|$. To $O((b\xi)^2)$, we find $\alpha^2_\mathrm{min} \approx |d^2 + \delta_b| bX^2/(\kappa_\mathrm{b}\pi(1-X)^2)$. Since α is always limited by geometry, we can use this formula to estimate maximum internal forces δ_b that can be overcome by external forcing. Assuming $|\alpha_\mathrm{min}| < \pi/3$, $d^2 = 0$ and typical parameters employed above, we estimate $\delta_b \lesssim 16\,\mathrm{k_B T/nm}$. This maximum force scale is not large and membrane channels possibly have a less pronounced conical shape. Therefore, radial expansion in a weak-tension membrane is likely not favored by force, which is in contrast to conical deformation.

Interaction between channels.– Membrane deformation can lead to collective effects where force at one channel affects the gating of neighboring channels. For $F = 0$, the interaction between membrane inclusions has been studied extensively [43, 52–59]. We consider here two channels with radii $b_{\{1,2\}}$ and conical angles $\alpha_{\{1,2\}}$ that are separated by a distance R in a homogeneous membrane. A force F is applied to each channel. The membrane energy $\tilde{\mathcal{F}}_\mathrm{m}$ can be calculated approximately through a multipole expansion assuming $\xi b_{\{1,2\}} \ll 1$ and $R \gg b_{\{1,2\}}$, which is appropriate for $R \gtrsim 3b_1$ when $b_1 = b_2$ [60]. For the individual channels, we write the deformation energy given by Eq. (5) as $\tilde{\mathcal{F}}_{\mathrm{m},1}$ and $\tilde{\mathcal{F}}_{\mathrm{m},2}$, where the parameters b, α are substituted by $b_{\{1,2\}}$, $\alpha_{\{1,2\}}$. For the interaction energy $\tilde{\mathcal{F}}_{\mathrm{m,R}} \equiv \tilde{\mathcal{F}}_\mathrm{m} - \tilde{\mathcal{F}}_{\mathrm{m},1} - \tilde{\mathcal{F}}_{\mathrm{m},2}$ we find [34]

$$\tilde{\mathcal{F}}_{\mathrm{m,R}} \approx (\alpha_1 b_1 + \alpha_2 b_2) F K_0(\xi R) + 2\pi\gamma b_1 b_2 \alpha_1 \alpha_2 K_0(\xi R) + \sum_{i=1,2} F^2 b_i^2 \left(\frac{(1+2X_i)\, K_0(\xi R)}{16\kappa_\mathrm{b}\pi} + \frac{(1 - R\xi K_1(\xi R))^2}{8\pi R^2 \gamma} \right), \tag{7}$$

where $X_i = -\Gamma_e - \log(b_i\xi/2)$ and contributions of $O(b_i^2\xi/R, (b_i\xi)^2)$ as well as terms that do not depend on α_i, b_i are neglected. $K_n(x)$ are modified Bessel functions of the second kind. Interaction becomes significant when the distance R is smaller than the lengthscale ξ^{-1}.

To study the role of interactions for gating we focus on the simplest case, namely conical deformation of initially cylindrical channels ($\alpha_c = 0$ for both channels). Since both forces have the same sign, interaction increases the energy that can be released by conical deformation. Analogous to the analysis for a single channel, force thresholds F_2^* for combined conical deformation of two neighboring channels can be calculated from the condition $-|\partial_{\alpha_i} \mathcal{F}_\mathrm{m}|_0 + \delta_\alpha = 0$, $i \in \{1, 2\}$. Fig. 4 demonstrates

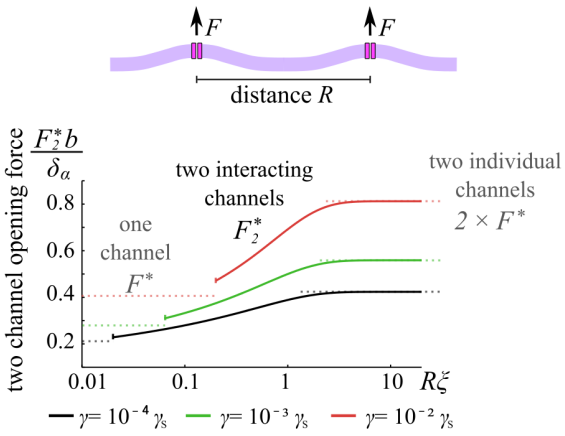

FIG. 4. Channel interaction can enhance force sensitivity. For close distances, $R\xi \ll 1$, the force necessary for conical deformation of two channels F_2^* is almost as small as for a single channel F^*. Lines end at the minimum distance $R = (b_1 + b_2)$. $b_{\{1,2\}} = 3\,\mathrm{nm}$, $\alpha_c = 0$, $\kappa_\mathrm{b} = 25\,\mathrm{k_B T}$, $\delta_\alpha = 180\,\mathrm{k_B T}/\pi$.

that force thresholds for conical deformation are significantly reduced by channel interaction. When $R \ll \xi^{-1}$, the force F^* that is necessary to deform a single channel almost suffices to deform two channels. Although membrane-mediated interactions are not pairwise additive, two-channel interaction is believed to be dominant for sparsely distributed proteins [55]. Consequently, we expect from Eq. (7) that force-sensitivity of a channel ensemble can be amplified by collective mechanics, which would allow a response to weak, local forces.

Experiments and predictions.– The theoretical framework laid out in this letter is generic since the membrane energy (1) affects gating of any deforming channel. Whether membrane energy dominates the gating process must be investigated for specific channels through experiments or molecular dynamics simulations. For both avenues, the theory provides helpful predictions and tools.

The current experimental status allows a few consistency tests. First, molecular structures [61, 62] indicate that radial deformation of known tethered channels is small, order 0.1 nm, but transmembrane units tilt during opening. This finding is in line with the above analysis, where conical channel deformations under force are favored by the membrane. Second, the observed activation of tethered TRP-channels through bilayer perturbations [30] supports a role of the membrane. Quantitative measurements of this type can be analyzed using Eq. (5) by calculating gating probabilities, which we describe in [34]. Third, the theory predicts that channel-channel interaction can lead to a sub-linear dependence of opening force on the number of tethered channels. This effect may be measurable at small tensions, e.g., by force application with an optical trap [3] when the tether den-

sity is varied biochemically [29].

Finally, we emphasize that tension sensing and force sensing via tethers are not mutually exclusive, but complimentary mechanisms. While tension sensing requires $\gamma \gtrsim 1\,\mathrm{k_B T/nm^2}$, force sensing requires $\gamma \lesssim 0.1\,\mathrm{k_B T/nm^2}$ and becomes rather ineffective at large tension. For illustration, we consider TREK-1, an established tension-sensitive channel [63] that nevertheless associates with the cytoskeleton [64, 65]. TREK-1 changes its conical angle $\alpha_c \simeq -0.2$ during gating as $\Delta\alpha \simeq 0.36$ while crossing a molecular energy barrier of $[4 - 7.7]\,\mathrm{k_B T}$ [66]. Gating occurs at tensions in the range of $[0.5 - 3]\,\mathrm{k_B T/nm^2}$. Using Eq. (5), we estimate that a cytoskeletal force of $|F| = 10\,\mathrm{pN}$ in the presence of gating-tension leads to energy changes $\sim 2\,\mathrm{k_B T}$, which is smaller than the energy barrier. However, for weak tension, $\gamma \sim 0.01\,\mathrm{k_B T/nm^2}$, deformation under force releases $\sim 7\,\mathrm{k_B T}$, which is clearly comparable to the gating energy barrier. We conclude that some tethered channels likely play a double role as force- and membrane-tension sensors.

We thank the NSF for support via grant MCB-1330288 (to Z. Gitai and H.A.S.) and the DAAD for a postdoctoral fellowship (to B.S.).

[1] M. Chalfie, Nat. Rev. Mol. Cell Bio. **10**, 44 (2009).
[2] B. Martinac, J. Cell Sci. **117**, 2449 (2004).
[3] K. Hayakawa, H. Tatsumi, and M. Sokabe, J. Cell Sci. **121**, 496 (2008).
[4] R. B. Bass, P. Strop, M. Barclay, and D. C. Rees, Science **298**, 1582 (2002).
[5] S. Sukharev and D. P. Corey, Sci. Signal. **2004**, re4 (2004).
[6] R. Phillips, T. Ursell, P. Wiggins, and P. Sens, Nature **459**, 379 (2009).
[7] N. Dan and S. A. Safran, Biophys. J. **75**, 1410 (1998).
[8] M. S. Turner and P. Sens, Phys. Rev. Lett. **93**, 118103 (2004).
[9] K.-J.-B. Lee, Phys. Rev. E **73**, 021909 (2006).
[10] X. Chen, Q. Cui, Y. Tang, J. Yoo, and A. Yethiraj, Biophys. J. **95**, 563 (2008).
[11] S. A. Rautu, G. Rowlands, and M. S. Turner, Phys. Rev. Lett. **114**, 098101 (2015).
[12] P. Wiggins and R. Phillips, Proc. Nat. Acad. Sci. **101**, 4071 (2004).
[13] V. Markin and F. Sachs, Phys. Biol. **1**, 110 (2004).
[14] D. Reeves, T. Ursell, P. Sens, J. Kondev, and R. Phillips, Phys. Rev. E **78**, 041901 (2008).
[15] O. S. Pak, Y.-N. Young, G. R. Marple, S. Veerapaneni, and H. A. Stone, Proc. Nat. Acad. Sci. **112**, 9822 (2015).
[16] H. W. Huang, Biophys. J. **50**, 1061 (1986).
[17] P. Helfrich and E. Jakobsson, Biophys. J. **57**, 1075 (1990).
[18] C. Kung, Nature **436**, 647 (2005).
[19] A. W. Orr, B. P. Helmke, B. R. Blackman, and M. A. Schwartz, Dev. Cell **10**, 11 (2006).
[20] B. Martinac, Biochim. Biophys. Acta **1838**, 682 (2014).
[21] N. Tavernarakis and M. Driscoll, Annu. Rev. Physiol. **59**, 659 (1997).
[22] R. O'Hagan, M. Chalfie, and M. B. Goodman, Nat. Neurosci. **8**, 43 (2005).
[23] J. Howard and S. Bechstedt, Curr. Biol. **14**, R224 (2004).
[24] P. Delmas and B. Coste, Cell **155**, 278 (2013).
[25] C. Liu and C. Montell, Biochem. Biophys. Res. Com. **460**, 22 (2015).
[26] W. Zhang, L. E. Cheng, M. Kittelmann, J. Li, M. Petkovic, T. Cheng, P. Jin, Z. Guo, M. C. Göpfert, L. Y. Jan, *et al.*, Cell **162**, 1391 (2015).
[27] M. Sotomayor, D. P. Corey, and K. Schulten, Structure **13**, 669 (2005).
[28] L. Li, S. Wetzel, A. Plückthun, and J. M. Fernandez, Biophys. J. **90**, L30 (2006).
[29] M. Prager-Khoutorsky, A. Khoutorsky, and C. W. Bourque, Neuron **83**, 866 (2014).
[30] K. Hill and M. Schaefer, J. Biol. Chem. **282**, 7145 (2007).
[31] T. M. Suchyna, S. E. Tape, R. E. Koeppe, O. S. Andersen, F. Sachs, and P. A. Gottlieb, Nature **430**, 235 (2004).
[32] F. Khalili-Araghi, J. Gumbart, P.-C. Wen, M. Sotomayor, E. Tajkhorshid, and K. Schulten, Curr. Opin. Struct. Biol. **19**, 128 (2009).
[33] W. Rawicz, K. Olbrich, T. McIntosh, D. Needham, and E. Evans, Biophys. J. **79**, 328 (2000).
[34] See supplemental material.
[35] J. Dai and M. P. Sheetz, Biophys. J. **77**, 3363 (1999).
[36] D. Raucher and M. P. Sheetz, Biophys. J. **77**, 1992 (1999).
[37] I. Derényi, F. Jülicher, and J. Prost, Phys. Rev. Lett. **88**, 238101 (2002).
[38] M. Jablin, K. Akabori, and J. Nagle, Phys. Rev. Lett. **113**, 248102 (2014).
[39] M. Ø. Jensen and O. G. Mouritsen, Biochim. Biophys. Acta **1666**, 205 (2004).
[40] O. S. Andersen and R. E. Koeppe, Annu. Rev. Biophys. Biomol. Struct. **36**, 107 (2007).
[41] F. MacKintosh and T. Lubensky, Phys. Rev. Lett. **67**, 1169 (1991).
[42] U. Seifert, J. Shillcock, and P. Nelson, Phys. Rev. Lett. **77**, 5237 (1996).
[43] J.-B. Fournier, Eur. Phys. J. E **11**, 261 (1999).
[44] Y. Kozlovsky, J. Zimmerberg, and M. M. Kozlov, Biophys. J. **87**, 999 (2004).
[45] S. May, Y. Kozlovsky, A. Ben-Shaul, and M. Kozlov, Eur. Phys. J. E **14**, 299 (2004).
[46] P. I. Kuzmin, S. A. Akimov, Y. A. Chizmadzhev, J. Zimmerberg, and F. S. Cohen, Biophys. J. **88**, 1120 (2005).
[47] M. Venturoli, M. M. Sperotto, M. Kranenburg, and B. Smit, Phys. Rept. **437**, 1 (2006).
[48] M. C. Watson, A. Morriss-Andrews, P. M. Welch, and F. L. Brown, J. Chem. Phys. **139**, 084706 (2013).
[49] D. Argudo, N. P. Bethel, F. V. Marcoline, and M. Grabe, Biochim. Biophys. Acta (2016).
[50] C. Nielsen, M. Goulian, and O. S. Andersen, Biophys. J. **74**, 1966 (1998).
[51] T. Ursell, J. Kondev, D. Reeves, P. A. Wiggins, and R. Phillips, in *Mechanosensitive Ion Channels* (Springer, 2008) pp. 37–70.
[52] M. Goulian, R. Bruinsma, and P. Pincus, Europhys. Lett. **22**, 145 (1993).
[53] R. R. Netz and P. Pincus, Phys. Rev. E **52**, 4114 (1995).
[54] T. R. Weikl, M. M. Kozlov, and W. Helfrich, Phys. Rev. E **57**, 6988 (1998).
[55] T. Chou, K. S. Kim, and G. Oster, Biophys. J. **80**, 1075

(2001).
[56] A. R. Evans, M. S. Turner, and P. Sens, Phys. Rev. E **67**, 041907 (2003).
[57] M. M. Müller, M. Deserno, and J. Guven, Europhys. Lett. **69**, 482 (2005).
[58] C. A. Haselwandter and R. Phillips, Europhys. Lett. **101**, 68002 (2013).
[59] J.-B. Fournier, Phys. Rev. Lett. **112**, 128101 (2014).
[60] B. J. Reynwar and M. Deserno, Soft Matter **7**, 8567 (2011).
[61] C. E. Paulsen, J.-P. Armache, Y. Gao, Y. Cheng, and D. Julius, Nature **520**, 23 (2015).
[62] E. Cao, M. Liao, Y. Cheng, and D. Julius, Nature **504**, 113 (2013).
[63] S. G. Brohawn, Z. Su, and R. MacKinnon, Proc. Nat. Acad. Sci. **111**, 3614 (2014).
[64] I. Lauritzen, J. Chemin, E. Honore, M. Jodar, N. Guy, M. Lazdunski, and A. J. Patel, EMBO rept. **6**, 642 (2005).
[65] C. D. Cox, C. Bae, L. Ziegler, S. Hartley, V. Nikolova-Krstevski, P. R. Rohde, C.-A. Ng, F. Sachs, P. A. Gottlieb, and B. Martinac, Nature **7** (2016).
[66] G. Maksaev, A. Milac, A. Anishkin, H. R. Guy, and S. Sukharev, Channels **5**, 34 (2011).